Measurement and correlation of high frequency behaviors of a very flexible beam undergoing large deformation [†]

Jae Wook Lee[1], Hyun Woo Kim[1], Hi Chun Ku[1] and Wan Suk Yoo[2,*]

[1]*Department of Mechanical Engineering, Pusan National University, Busan, 609-735, Korea*
[2]*School of Mechanical Engineering, Pusan National University, Busan, 609-735, Korea*

Abstract

A correlation method of high frequency behaviors of a very flexible beam undergoing large displacement is presented. The suggested method based on the experimental modal analysis leads to more accurate correlation results because it directly uses the modal parameters of each mode achieved from experiment. First, the modal testing and the parameter identification method are suggested for flexible multibody dynamics. Due to the flexibility of a very thin beam, traditional testing methods such as impact hammer or contact type accelerometer are not working well. The suggested measurement with high speed camera, even though the test beam is very flexible, is working well. Using measurements with a high speed camera, modal properties until the 5th mode are measured. And After measuring each damping ratio until the 5th mode, a generic damping model is constructed using inverse modal transformation technique. It's very interesting that the modal transformation technique can be also applied even in the ANCF simulation which uses the global displacement and finite slope as the nodal coordinates. The results of experiment and simulation are compared until the 5th mode frequency, respectively, by using ANCF forced vibration analysis. Through comparison between numerical simulation and experiment, this study showed that the proposed generic damping matrix, modal testing and parameter identification method is very proper in flexible multibody dynamic problems undergoing large deformation.

Keywords: Absolute nodal coordinate formulation; Experimental modal testing; Generic damping model; High frequency behavior

---

1. Introduction

From the first introduction of the absolute nodal coordinate formulation (ANCF) [1, 2], there have been many researches that study dynamic motions of large deformable structures using the ANCF. Compared to other finite element formulations, such as floating reference formulation and incremental finite element approach [1], the element with the ANCF can represent arbitrary large deformations more easily because it use finite slopes as nodal variables from the

inertial frame. And the equations of motion contain a constant mass matrix and a constant vector of generalized gravity forces as well as zero centrifugal and Coriolis inertial forces. Thus, the ANCF is well known as a proper formulation to simulate large deformable structures in the flexible multi-body dynamics.

It is true that there have been numerous papers to verify their large deformable models with experiments [3-6]. But, none have focused on high frequency behaviors of their flexible structures. They studied only the fundamental frequency; moreover, there is no trial to compare their high frequency behaviors to experimental results. Within the knowledge of the author, this study is the first trial to correlate the

results of high mode simulations with those of experiment.

In this study, the correlation method of high frequency behaviors of a flexible beam undergoing large oscillation is presented. The method, which is based on experimental modal analysis [7, 8], leads to obtaining more accurate correlation results because it directly uses the modal parameters of each mode achieved from experiment. First, modal testing and the parameter identification method are suggested for the flexible multibody dynamics. Due to the flexibility of a very thin beam, traditional modal testing methods are not working well. It's very tedious to remove the double hammering effects, the cancellation of mass of contact type accelerator and bad coherence performance of non-contact type accelerometers. But, even though the test beam is very flexible, the suggested method works well. This method uses the damped decay behavior of free vibrating beam and a high speed camera to capture the motion of the beam instead of accelerometers. And modal properties until the 5th mode are calculated by using motion tracking method and 1 DOF identification method.

In previous studies [3-6, 9, 12], the linear damping model is widely used for simplicity and efficiency. But, it is impossible for the linear damping model to predict high order behaviors because there are only two frequency dependent constraints. Garcia-Vallejo [10] suggested the internal damping model based on linear visco-elasticity theory for the ANCF. He made an effort to make a damping model which can express no energy dissipation under rigid body motion and it is indeed good approach in structural dynamics as well as multibody dynamics simulation. But because of their thin structure in large deformation analysis, external damping is more important than internal damping in most mechanical application except hyperelastic or viscoelastic materials. So, it is necessary to find a new damping model which can express both internal and external damping characteristics. In this study, a frequency-dependent generic damping model based on experimental modal analysis is also introduced for flexible multibody dynamics [7, 8]. The generic damping model is constructed using inverse modal transformation technique. It's very interesting that the modal transformation technique can be also applied even in the ANCF simulation which uses the global displacement and finite slope as the nodal coordinates.

Finally, the results of experiment and simulation

are compared until the 5th mode of the beam, respectively, by using ANCF forced vibration analysis. Then it is discussed that there are good agreements between experiment and simulation behaviors in spite of relatively high frequencies.

2. Physical experiments

2.1 Experimental setup and testing

The choice of material is very important in the large deformation test. During the large deformation, the behavior of the test material has to remain within the elastic limit. In this research, a thin spring-steel beam heat-treated to increase its strength and durability is selected. The sectional properties of the beam are shown in Table. 1.

Contact type accelerometers have been used to measure the response of the beam in traditional modal testing. But, in the large displacement and deformation test, it is difficult to attach a contact type accelerometer to the beam due to high flexibility of the beam. In this experiment, the fundamental frequency of the test beam is only 1.85Hz. Therefore, a high-speed camera is used to capture the motion instead of accelerometers. A high-speed camera, REDLAKE Motion Scope 1000s shown in Fig. 1, is used in this study. The target point is attached to the test beam to track the beam displacement. But even with a high speed camera and marker tracking method, it is very difficult to measure the high order mode of the beam with high velocity. It is prone to losing the tracking point in the same methodology as previous researches. This is the reason why so many researchers have been focused only on the fundamental frequency.

In this paper, the concept of global parameter of damping ratio to measure the high frequency behavior is used. The vibration signal made by LabVIEW is transferred to the Exciter by using a PXI 4461 board. Fig. 2 shows the PXI 4461 board generating sinusoidal function and the exciter, LMT-100, produced by Ling Electronics. It can produce output force to 100 lb (444.8 N) and has maximum displacement of 1 inch (25.4 mm) and 2000 Hz. The large deformation experimental setup for the beam is constructed as shown in Fig. 3. The beam is located on the vertical direction and excited along the horizontal direction when it is on the equilibrium state due to the gravity. The movements of the markers are captured by the high speed camera and are traced by a data acquisition system.

Table 1. Standard properties of the beam.

Length (mm)	Width (mm)	Thickness (mm)	Density (kg/m³)	Elastic modulus (MPa)
500	5.0	0.50	8000.0	210,000

Fig. 1. High speed camera.

Fig. 2. PXI 4461 board generating excitation (left) and Exciter (right).
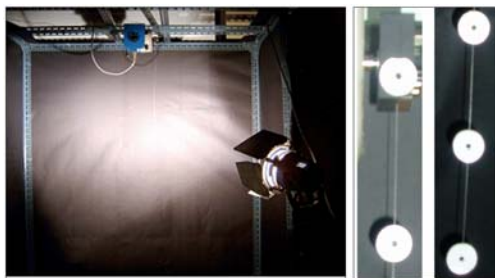
Fig. 3. Experimental setup for large deformation measurement and markers attached to the test beam.

2.2 Modal testing and identification

In the experimental modal analysis, steady state or transient response test is widely used to get the modal characteristics. They use a harmonic base excitation or impact hammer as excitation, respectively. And contact or non-contact type accelerometers are widely used to get the experimental data.

But, in the large deformation beam test, the mass of
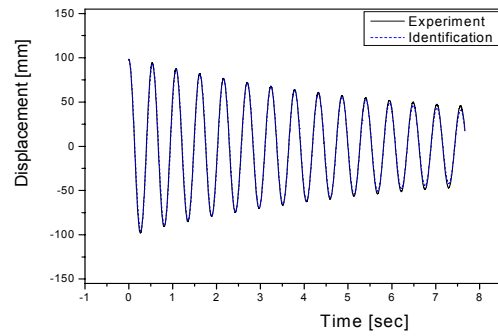
Fig. 4. Identification results of 1st mode: 1.85 [Hz].
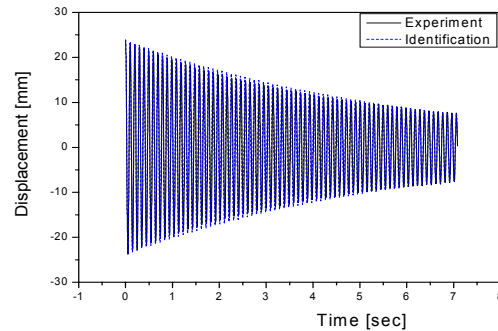
Fig. 5. Identification results of 2nd mode: 10.19 [Hz].
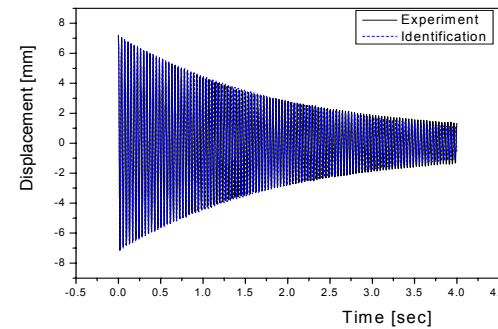
Fig. 6. Identification results of 3rd mode: 26.84 [Hz].
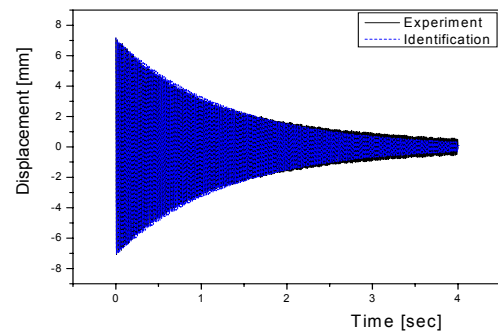
Fig. 7. Identification results of 4th mode: 53.22 [Hz].

Table 2. Identified modal parameters from experiments.

	Natural frequency (Hz)	Damping ratio (%)
1st mode	1.85	1.00
2nd mode	10.19	0.28
3rd mode	26.84	0.28
4th mode	53.20	0.23
5th mode	88.60	0.30

Fig. 8. Identification results of 5th mode: 88.60 [Hz].

accelerometer can affect the response of the beam. Thus a non-contact type such as a laser accelerometer cannot guarantee a constant measuring point due to large displacement, which makes bad cohe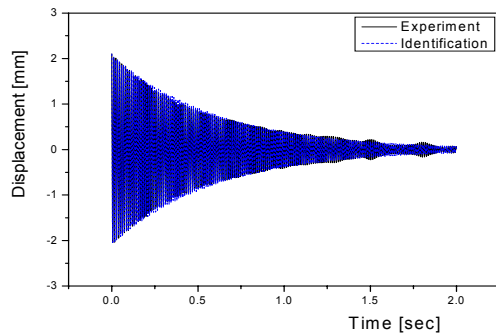rence in the modal testing. Because the beam is very flexible and has a small mass, double hammering or non-impact force also leads to bad results.

Because of these reasons, it is very difficult to get the modal parameters using traditional methods in a large displacement beam test.

For a large deformation test, another test procedure is required. In this study, a damped decay test of free vibrating beam is suggested as a proper test procedure. The beam is located on the vertical direction and is excited along the horizontal direction with their natural frequencies until a steady state behavior occurs. When the beam reaches to a steady-state, a sudden drop of the excitation makes the beam vibrate with its natural properties. And then the natural frequency and damping ratio can be found with Eq. (1), which is a 1 D.O.F. free vibration equation.

$$x(t) = e^{-\zeta \omega_n t} \left(x_0 \cos(\omega_d t) + \frac{\dot{x}_0 + \zeta \omega_n x_0}{\omega_d} \sin(\omega_d t) \right) \quad (1)$$

where $\omega_d = \omega_n \sqrt{1-\zeta^2}$ is the damped natural frequency.

The modal parameters to be calculated are the values which the residue between Eq. (1) and test data is minimized such as Eq. (2).

$$\text{Min. } \Re(\omega_r, \zeta_r) = \sqrt{\sum_{i=0}^{n} (x_{\exp} - x_{\text{ide}})^2} \quad (2)$$

Figs. 4-8 show the damped behaviors of the beam from the 1st to the 5th natural frequency, respectively; Table 2 shows the resultant natural frequencies and damping ratios identified from the physical experiments.

3. Simulation with ANCF

3.1 Equations of motion of 2D beam

Fig. 8 shows a finite element model of the 2D Euler-Bernoulli beam. The center line is parameterized by the value $p = 0, \dots, l$, where, l is the initial length of the beam element. The vector of the absolute nodal coordinate consists of two vectors. One is a position vector of the both ends, r_0, r_l, and another is a tangent slope vector of the both ends, τ_o, τ_l, respectively [1, 3].

Therefore, Eq. (3) is the vector of the absolute nodal coordinates of the beam.

$$\mathbf{e} = \begin{Bmatrix} r_0 \\ \tau_0 \\ r_l \\ \tau_l \end{Bmatrix} = \begin{Bmatrix} e_1 \\ e_2 \\ e_3 \\ e_4 \end{Bmatrix} \quad (3)$$

It can be shown that the position of an arbitrary point on the element is given by Eq. (4).

$$\mathbf{r}(p) = \begin{bmatrix} s_1 & 0 & s_2 & 0 & s_3 & 0 & s_4 & 0 \\ 0 & s_1 & 0 & s_2 & 0 & s_3 & 0 & s_4 \end{bmatrix} \begin{Bmatrix} \begin{Bmatrix} r_{0x} \\ r_{0y} \end{Bmatrix} \\ \vdots \\ \begin{Bmatrix} \tau_{lx} \\ \tau_{ly} \end{Bmatrix} \end{Bmatrix} \quad (4)$$

Then, a global shape function is defined as Eq. (5).

$$s_1 = 1 - 3\xi^2 + 2\xi^3, \quad s_2 = l(\xi - 2\xi^2 + \xi^3),$$
$$s_3 = 3\xi^2 - 2\xi^3, \quad s_4 = l(\xi^3 - \xi^2) \quad (5)$$

where $\xi = p/l$ is a non-dimensional variable. For the sake of simplicity, a slightly different notation is

applied to the same equations.

$$\mathbf{r}(p) = \begin{bmatrix} s_1\mathbf{I} & s_2\mathbf{I} & s_3\mathbf{I} & s_4\mathbf{I} \end{bmatrix} \begin{Bmatrix} \mathbf{e}_1 \\ \mathbf{e}_2 \\ \mathbf{e}_3 \\ \mathbf{e}_4 \end{Bmatrix} = \sum_{k=1}^{4} s_k\mathbf{e}_k \qquad (6)$$

where $\mathbf{I}$ represents the 2×2 identity matrix. The equations of motion of the beam element can be obtained from the following Lagrange Eqs. [11].

$$\frac{d}{dt}\left(\frac{\partial T}{\partial \dot{\mathbf{e}}}\right)^T - \left(\frac{\partial T}{\partial \mathbf{e}}\right)^T + \left(\frac{\partial U}{\partial \mathbf{e}}\right)^T = \left(\frac{\delta W}{\delta \mathbf{e}}\right)^T \qquad (7)$$

where,

$$T = \tfrac{1}{2}\int_0^l \mu \dot{\mathbf{r}}^T \dot{\mathbf{r}}\, dp$$
$$\delta W = \int_0^l \delta\mathbf{r}^T \mu \mathbf{g}\, dp \qquad (8)$$

And T is the kinetic energy, U is the strain energy by internal force. δW is the virtual work of external forces. And μ is the linear mass density.

After substituting Eq. (8) into Eq. (7), rearrange the equation in matrix form,

$$\mathbf{M}\ddot{\mathbf{e}} + \mathbf{Q}^e = \mathbf{Q}^g \qquad (9)$$

where,

$$\mathbf{M} = \frac{\mu l}{420}\begin{bmatrix} 156\mathbf{I} & & & sym. \\ 22l\mathbf{I} & 4l^2\mathbf{I} & & \\ 54\mathbf{I} & 13l\mathbf{I} & 156\mathbf{I} & \\ -13l\mathbf{I} & -3l^2\mathbf{I} & -22l\mathbf{I} & 4l^2\mathbf{I} \end{bmatrix} \qquad (10)$$

And

$$\mathbf{Q}^e = \begin{Bmatrix} \mathbf{Q}_1^e \\ \mathbf{Q}_2^e \\ \mathbf{Q}_3^e \\ \mathbf{Q}_4^e \end{Bmatrix}, \quad \mathbf{Q}^g = \begin{Bmatrix} \mu\mathbf{g}l/2 \\ \mu\mathbf{g}l^2/12 \\ \mu\mathbf{g}l/2 \\ -\mu\mathbf{g}l^2/12 \end{Bmatrix} \qquad (11)$$

The block element of the mass matrix $\mathbf{M}_{ij}$ and the vectors of generalized gravity forces $\mathbf{Q}_i^g$ are defined as follows.

$$\mathbf{M}_{ij} = \frac{\partial^2 T}{\partial \dot{\mathbf{e}}_i \partial \dot{\mathbf{e}}_j^T} = \mu \underbrace{\int_0^l s_i s_j\, dp}_{M_{ij}}\, \mathbf{I} = M_{ij}\mathbf{I}$$
$$\mathbf{Q}_i^g = \frac{\delta W}{\delta \mathbf{e}_i} = \mu\mathbf{g}\int_0^l s_i\, dp, \quad i,j = 1,\dots,4 \qquad (12)$$

To calculate the vectors of generalized elastic forces, $\mathbf{Q}_i^e = \partial U / \partial \mathbf{e}_i$ is very cumbersome because of the complexity of the strain energy term U.

So, the strain energy is divided into tensile and flexural components as Eq. (13).

$$U = U^\varepsilon + U^\kappa = \frac{1}{2}\int_0^l EA\varepsilon^2 dp + \frac{1}{2}\int_0^l EI\kappa^2 dp \qquad (13)$$

where ε represents the longitudinal deformation and κ represents the transverse curvature. The tensile stiffness EA and the flexural stiffness EI are assumed to be constant throughout the beam element. More detailed derivation for the equations of motion and several models of elastic forces are well explained in Ref. [3, 11].

3.2 Optimization for frequency matching

From the author's knowledge, most researchers have focused on correlating their results with experiment at only the fundamental mode. The 1st mode with the lowest frequency is relatively easy to correlate the results of simulation with those of experiment because the frequency which has to be correlated is only one. But, in higher order modes, the natural characteristics of the beam can highly affect the response of the forced vibration behavior. All frequencies among a specific frequency band have to be correlated at the same time. In this study, because spring-steel that has been heat treated is used, there is no guarantee that the natural properties of simulation coincide with those of experiment. Table 3 shows the difference of natural frequencies in the case of using standard properties of steel.

In the case of standard beam properties, the difference between measurement and simulation is almost by 10 % even the 1st mode due to above reason. It must be affecting on the dynamic simulation very seriously. So, the optimization process was carried out to find the proper material properties. The beam used in this study has 20 finite elements, 84 coordinates and 4 constraint equations. In the optimization process, design variables are selected as the width and height of each beam element and elastic modulus and density. The variance of those design variables is limited within 10 %. To correlate with natural characteristics, the objective function is chosen to minimize the residue of natural frequencies and modes from the 1st to the 5th mode similar to Eq. (2) in section 2.2. The resultant design variables are listed in Table 4.

Table 3. Optimized results for frequency matching.

Natural Freq.	Test (Hz)	Simulation [Hz]	
		Before optimization	After optimization
1st mode	1.85	1.67	1.84
2nd mode	10.19	10.47	10.18
3rd mode	26.84	29.32	26.81
4th mode	53.20	57.46	53.15
5th mode	88.60	94.97	88.79

Table 4. Optimum properties of the beam.

Length (mm)	Width (mm)	Thickness (mm)	Density (kg/m^3)	Elastic modulus (MPa)
500	5.0	0.49	8108.0	205,130

4. Choice of damping model

4.1 Linear damping model

To Consider effects of internal and external dissipation, a linear damping model is widely used in structural dynamics problem for the sake of simplicity.

$$\mathbf{Q^{damp}} = \mathbf{C}\dot{e} \tag{14}$$

In this model, a particular form of proportional Rayleigh damping is implemented such as Eq. (15).

$$\mathbf{C} = \alpha\mathbf{M} + \beta\mathbf{K} \tag{15}$$

where $\mathbf{M}$ is a mass matrix and $\mathbf{K}$ is a stiffness matrix.

$$\alpha = \frac{2\omega_1\omega_2(\zeta_1\omega_2 - \zeta_2\omega_1)}{\omega_2^2 - \omega_1^2}, \ \beta = \frac{2(\zeta_2\omega_2 - \zeta_1\omega_1)}{\omega_2^2 - \omega_1^2} \tag{16}$$

$$\ddot{e}_r + 2\zeta_r\omega_r\dot{e}_r + \omega_r^2 e_r = 0 \tag{17}$$

Values α, β depend on frequencies ω_1 and ω_2 as well as on damping ratios ζ_1 and ζ_2 for the first two modes of the system that appear in the modal dynamic equations, Eq. (17).

But, the drawback of the linear damping model is just to control damping of a beam with only two modes because the constraint parameters are only two, α and β. And if the parameters are changed to correlate higher motions, it is certain that the low frequency motions will be different. The ratios ζ_1 and ζ_2

Table 5. Proportional damping parameters.

ω_1 (Hz)	ω_2 (Hz)	ζ_1 (%)	ζ_2 (%)	α	β
1.85	10.19	1.0	0.28	0.228	3.18E-4

can be calculated from identified data in the previous section. Table 5 shows the resultant damping parameters calculated for computer simulations. In Eq. (18), one can easily verify that α controls the low frequency damping and β controls the high frequency damping. In Table 4, The value of α is much larger than that of β. But, because the role of α is to dissipate only fundamental frequency and beat frequencies of higher modes, parameter β has more influence on the motion of the high order responses of the beam.

$$\zeta_r = \frac{\alpha + \beta\omega_r^2}{2\omega_r} = \frac{\alpha}{2\omega_r} + \frac{\beta\omega_r}{2} \tag{18}$$

4.2 Generic damping model

In the previous section, one can see that it is impossible to correlate the high frequency behavior of the structure by using the linear damping model. The linear damping model can express the motion of only a maximum two frequencies. So, a new damping model which can have frequency dependent properties and express the independent high frequency damping characteristic is necessary. In this study, a frequency dependent generic damping model based on inverse modal transformation technique is also introduced into flexible multibody dynamics [7, 8].

From the identified modal parameters in section 2.2, the generic damping matrix can be derived by using the modal transformation technique. Modal transformation is the transformation from an identified damping matrix in the frequency domain to general damping matrix in physical time domain using modal vector. With the undamped natural modal matrix $\mathbf{\Phi}$, one can calculate the generic viscous damping matrix using orthogonal properties, as shown in Eq. (19). Eq. (19) shows the modal transformation of generic damping matrix. Eq. (20) is an inverse modal transformation.

$$\mathbf{C}_g = \mathbf{\Phi}^T\mathbf{C}\mathbf{\Phi} \tag{19}$$

$$\mathbf{C} = \mathbf{\Phi}^{-T}\mathbf{C}_g\mathbf{\Phi}^{-1} = \mathbf{\Phi}^{-T}\mathrm{diag}\left[2\zeta_r\omega_r\right]\mathbf{\Phi}^{-1} \tag{20}$$

where $r = 1, \cdots, n$ and $\mathrm{diag}\left[2\zeta_r\omega_r\right]$ means the di-

agonal matrix of which its diagonal component is $2\zeta_r\omega_r$.

Using the mass normalization properties, one can derive the inverse modal matrix such as Eq. (22).

$$\mathbf{\Phi^T M \Phi = I} \qquad (21)$$
$$\mathbf{\Phi^{-T} = M\Phi}, \quad \mathbf{\Phi^{-1} = \Phi^T M} \qquad (22)$$

Substituting Eqs. (22) into Eq. (20), the generic damping model can be calculated as Eq. (23).

$$\mathbf{C = M\Phi}\mathrm{diag}\left[2\zeta_r\omega_r\right]\mathbf{\Phi^T M} \qquad (23)$$

where $\mathbf{M}$ is a mass matrix, $\mathbf{\Phi}$ is a mode shape vector and ζ_r, ω_r are critical damping ratio and natural frequency derived from modal parameter identification method, respectively.

5. Comparison of simulation and experiment

Experiment and simulation with base excitation are carried out from the 1st mode to the 5th mode. Using marker tracking method, displacement of the beam is measured. In Figs. 9-16, 'Experiment' means the measurement results of testing, 'Generic', blue dashed line, means the simulation results of the generic

damping model, and 'Linear', red dashed line, means the simulation results of the linear damping model.

Figs. 9 and 10 show the steady state and damped response of experiment and simulation at the 1st and 2nd mode frequencies, respectively. Both results are almost the same. So, one can know that the identified parameters give good results. Because the control parameters in the linear damping model are calculated from the first two modes, one can see that even the linear damping model can also predict the response well enough. Of course, the presented generic damping model also gives good correlation results.

Figs. 11-13 show the steady state and damped decay response of the 3th, 4th and 5th mode frequency, respectively. One can see that the linear damping model cannot predict the response of the beam well enough. Because there are no input parameters from the 3rd mode frequency in the linear damping model, the results from it are all arbitrary values. But, because the effect of β is dominant at high frequencies, the results of the linear damping model are prone to overestimate the damping characteristics compared to those of the experiments. The recalculated damping ratios from the simulation results of each damping model are listed in Table 6.
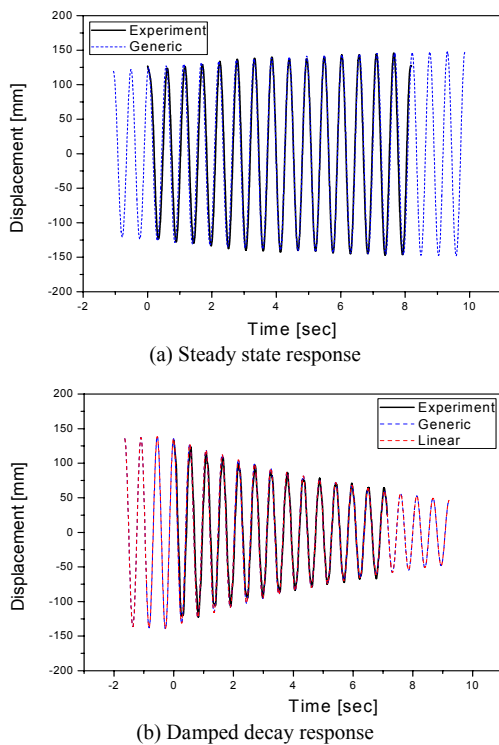

(a) Steady state response

(b) Damped decay response

Fig. 9. Comparison of experiment and simulation: 1st mode.

(a) Steady state response

(b) Transient decay response
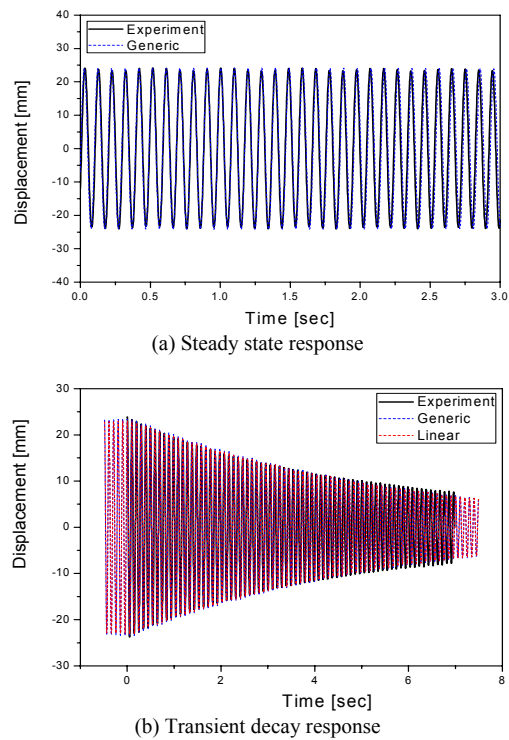
Fig. 10. Comparison of experiment and simulation: 2nd mode.

(a) Steady state response

(b) Transient decay response
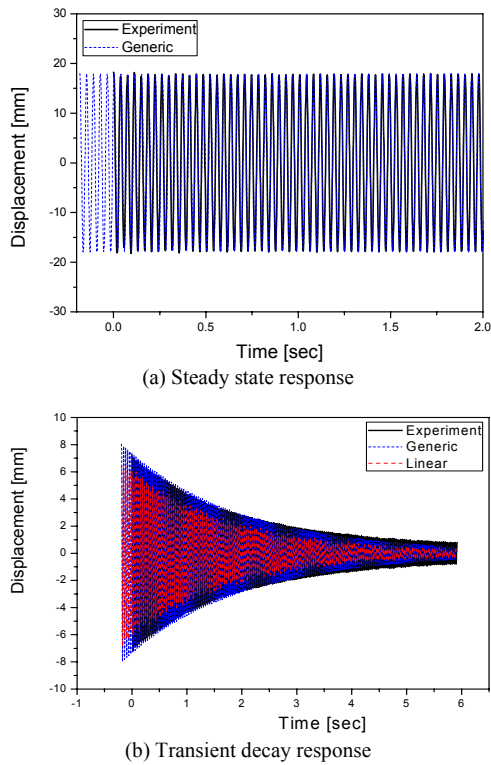
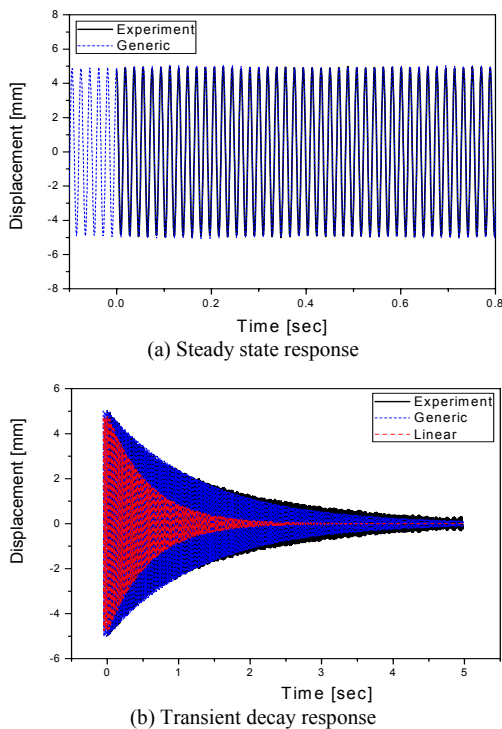Fig. 11. Comparison of experiment and simulation: 3rd mode.

Table 6. Resultant damping ratio of experiment and simulation.

	Damping ratio of each mode [%]				
	1st	2nd	3rd	4th	5th
Experiment	1.00	0.28	0.28	0.23	0.30
Generic	1.00	0.28	0.28	0.23	0.30
Linear	1.00	0.28	0.32	0.50	0.70

(a) Steady state response

(b) Transient decay response
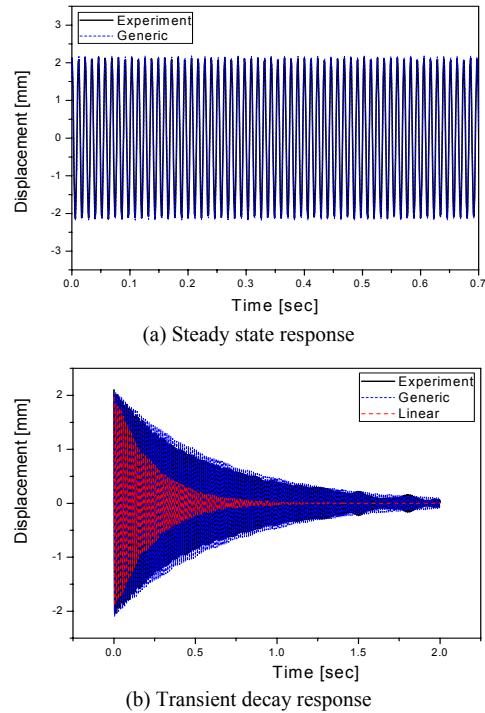
Fig. 13. Comparison of experiment and simulation: 5th mode.

One can understand that the damping ratios of the linear damping model are higher than those of physical experiment above the 3rd mode. Especially, the 5th damping ratio is different by about 57 %. Contrary to the linear damping model, the generic damping model can estimate the damping characteristics well enough in spite of the high frequency region because it directly uses the modal parameters of each mode achieved from experiment. If one can measure the modal parameters of the higher frequency, the generic damping model can control all frequency behavior which can be calculated.

Until now, it has been shown that the linear damping model cannot predict the response in high order behavior and the generic damping model which has the frequency dependent properties can predict the response well enough in spite of high frequencies.

(a) Steady state response

(b) Transient decay response

Fig. 12. Comparison of experiment and simulation: 4th mode.

5. Conclusion

Although there are many researches to study large deformable models, they all have focused only on the fundamental frequency. The measurement of high frequency is very difficult even with a high speed camera and node tracking methods. That's the reason why most researchers have focused on the 1st mode. And to correlate only the first mode, the linear damping model is sufficient. That's the reason why most of the previous researches adopt mass proportional damping because the parameter α is dominant at low frequency.

But, in high frequency, the experimental method and related damping model have to change. First, in this study, the proper modal testing and identification method are presented for flexible multibody dynamics by using the concept of global parameters. And the measuring of high frequency responses until the 5th mode, 89 Hz, has been done by proposed methods. This paper is the first research which studies the correlation of high order behaviors of a flexible beam with experiment results.

The study presents the proper correlation method with introducing the frequency dependent generic damping model. This research shows with the linear damping model, which is used traditionally for simplicity, it is impossible to express the high frequency motion at the same time, and the proposed generic damping model can suppress the number of frequency modes simultaneously. The absolute nodal coordinate formulation uses the global displacement and finite slope as nodal coordinates. So, this paper presents interesting results that the traditional modal damping theory can also be used even in the case of the nodal coordinates consisting of global displacement and finite slope. This paper shows that the modal transformation technique can be also applicable to a beam undergoing large displacements.

Finally, through comparisons between numerical simulation and experiment, this study shows that the presented generic damping matrix, modal testing and parameter identification method works well in flexible multibody dynamics undergoing large displacement.

Acknowledgment

References

[1] A. A. Shabana, Flexible Multibody Dynamics: Review of Past and Recent Developments, *Multibody System Dynamics*, 1 (1997) 189-222.

[2] A. A. Shabana, Dynamics of Multibody Systems, 3rd Edition, *Cambridge University Press*, Cambridge, 2005.

[3] W. S. Yoo, J. H. Lee, J. H. Sohn, S. J. Park, O. Dmitrochenko and D. Pogorelov, Large Oscillation of a thin cantilever beam: physical experiments and simulation, *Nonlinear Dynamics*, 34 (2003) 3-29.

[4] W. S. Yoo, S. J. Park, O. Dmitrochenko and D. Pogorelov, Verification of Absolute Nodal Coordinate Formulation in Flexible Multibody Dynamics via Physical Experiments of Large Deformation Problems, *Journal of Computational and Nonlinear Dynamics*, 1 (2006) 81-93.

[5] W. S. Yoo, J. H. Lee, J. H. Sohn, S. J. Park, O. Dmitrochenko and D. Pogorelov, Matching of Physical Experiments and Multibody Dynamic Simulation for Large Deformation Problems, *KSME International*, Vol. 18, No. 5 (2004) 742-752.

[6] W. S. Yoo, J. H. Lee, S. J. Park, J. H. Sohn, D. Poforelov and O. Dmitrochenko, Large Deflection Analysis of a Thin Plate: Computer Simulations and Experiments, *Multibody System Dynamics*, 11 (2004) 185-208.

[7] D. J. Ewins, Modal Testing: theory, practice and application, 2nd Edition, *Research Studies Press LTD.*, 2000.

[8] K. G. McConnell, Vibration Testing: Theory and Practice, *John Wiley & Sons*, Inc, 1995.

[9] Y. Takahashi, N. Shimizu, K. Suzuki, Introduction of Damping Matrix into Absolute Nodal Coordinate Formulation, W-1-1-4, *Proceedings of ACMD'02*, (2002).

[10] D. Garcia-Vallejo, J. Valverde and J. Dominguez, An Internal Damping Model for the Absolute Nodal Coordinate Formulation, *Nonlinear Dynamics*, 42, (2005) 347-369.

[11] M. Berzeri, A. A. Shabana, Development of simple models for the elastic forces in the absolute nodal coordinate formulation, *Journal of Sound and Vibration*, 235, 4 (2000) 539-565.

[12] Y. Takahasi, N. Shimizu and K. Suzuki, Study on the frame structure modeling of the beam element

formulated by absolute nodal coordinate approach, *Journal of Mechanical Science and Technology, 19*, 1 (2005) 283-291.

Jae-Wook Lee received his B.S. degree from Pusan National University (1999), M.S. from Pusan National University (2001). And he is currently a graduate student for the Ph.D. in Pusan National University. His major area is a flexible multi-body dynamics and structural dynamics based on FEM.

Wan-Suk Woo received his B.S. degree from Seoul National University (1976), M.S. from KAIST (1978) and Ph.D. from University of Iowa (1985). He is currently a Professor at the School of Mechanical Engineering at Pusan National University, and currently serving as a vice president in KSME. His major area is vehicle dynamics and flexible multibody dynamics.